Cluster Compounds

Deutsche Ausgabe: DOI: 10.1002/ange.201603374
Internationale Ausgabe: DOI: 10.1002/anie.201603374

$[(Me_3Si)Si]_3EtGe_9Pd(PPh_3)$, a Pentafunctionalized Deltahedral Zintl Cluster: Synthesis, Structure, and Solution Dynamics

*Feng Li, Alvaro Muñoz-Castro, and Slavi C. Sevov**

Abstract: *The title compound, which has a ten-atom deltahedral cluster core of Ge_9Pd, was synthesized through insertion of $Pd(PPh_3)$ into the tetrasubstituted nona-germanium cluster $[(Me_3Si)Si]_3EtGe_9$ through a reaction of the latter with $Pd(PPh_3)_4$. This first reaction of neutral tetrasubstituted nine-atom clusters shows that they retain reactivity despite their neutral charge. The Ge_9Pd core is the first that incorporates a 5-connected transition metal other than from Group VI, a noble metal in this case. Single-crystal X-ray diffraction shows that the ten-atom core is a closo-cluster with the expected shape of a bicapped square antiprism. ^1H and ^{13}C NMR spectroscopy show that, in contrast to the parent tetra-substituted $[(Me_3Si)Si]_3EtGe_9$, the new compound does not exhibit dynamics. Relativistic DFT calculations are used to explain the differences.*

Functionalization of nine-atom deltahedral germanium clusters with various organic and main-group fragments has become a very rich field in the chemistry of Zintl ions.[1] In turn, the resulting functionalized species are of interest for follow-up reactions. The reactivity of the hypersilyl trisubstituted nine-atom germanium monoanion $[Ge_9R_3]^-$ (**1**), where R is the hypersilyl group $Si(SiMe_3)_3$, has been extensively investigated since its initial synthesis in 2003.[2] It turned out that the anion can coordinate to a number of transition metals in various ways, thus making it a flexible ligand, both structurally and electronically.[3] In addition, mild oxidation with $FeCl_2$ resulted in formation of the neutral "dimer" $[Ge_{18}R_6]^0$ with a rearranged cluster core.[4] Not long ago, we reported a different approach for synthesis of the anion in nearly quantitative yields.[5] This made the species much more readily available in large amounts for further reactivity studies. We showed that $[Ge_9R_3]^-$ can also react with main-group organometallics and their halides, as well as with organic halides, to add a fourth substituent and form neutral tetrafunctionalized clusters $[Ge_9R_3R']^0$ (**2**), where $R' = SnPh_3$, Sn^nBu_3, Et, etc.[6] Our recent studies have shown that some of these neutral species exhibit interesting solution dynamics that resembles those observed before for substituted and/or centered Sn_9 and Pb_9 clusters.[7] The nature of the dynamics in **2** was suggested previously but has not been confirmed experimentally.[6b] In addition, the question of the reactivity of the neutral species Ge_9R_3R' compared to the parent monoanion $[Ge_9R_3]^-$ had not been addressed. Herein, we report the results of such studies, in which Ge_9R_3Et (**2**) is reacted with $Pd(PPh_3)_4$ to insert a $Pd(PPh_3)$ fragment into the cluster core to form $Ge_9R_3EtPd(PPh_3)$ (**3**), thereby unraveling the different reactivity caused by the presence of the ethyl substituent and the neutrality of **2**. The new compound represents the first example of a pentafunctionalized neutral deltahedral cluster, in this case a 10-atom *closo*-cluster core of Ge_9Pd with a 5-connected noble-metal atom. In addition, investigation of the solution properties of **3** helped clarify the nature of the solution dynamics of **2**.

Cluster **3** was prepared by treating a benzene solution of **2** with $Pd(PPh_3)_4$. After removal of the solvent under vacuum, the resulting brown-red solid was extracted with hexane. A large amount of brown block crystals of **3** (77% yield) were obtained after storing the solution at −20 °C for three days. The new compound, just like the parent **2**, is highly soluble in nonpolar solvents such as benzene, toluene, and hexanes (for experimental details, see the Supporting Information).

Cluster **3** is best described as a pentafunctionalized 10-atom *closo*-deltahedron of $[Ge_9Pd]$ (Figure 1). The five

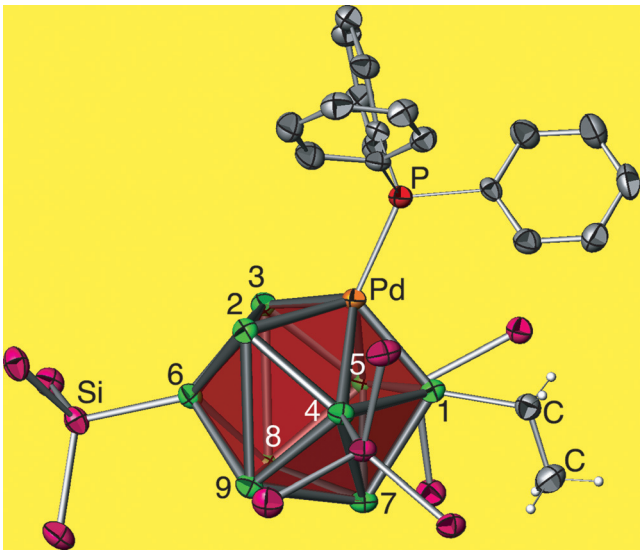

Figure 1. The structure of **3**, with a cluster core consisting of a bicapped square antiprism (Ge atoms shown in green and numbered): atoms 1 and 6 are capping, atoms 2-3-8-9 and 4-Pd-5-7 form the two squares of the antiprism. The hypersilylmethyl groups and the phenyl hydrogen atoms are omitted for clarity.

[*] Dr. F. Li, Prof. S. C. Sevov
Department of Chemistry and Biochemistry
University of Notre Dame, Notre Dame, IN 46556 (USA)
E-mail: ssevov@nd.edu
Homepage: http://www.nd.edu/~ssevov
Dr. A. Muñoz-Castro
Lab. de Química InorgánicayMateriales Moleculares
Universidad Autonoma de Chile
Llano Subercaceaux 2801, San Miguel, Santiago (Chile)
Supporting information and the ORCID identification number(s) for the author(s) of this article can be found under http://dx.doi.org/10.1002/anie.201603374.

functionalities are an *exo*-bonded ethyl moiety, three hypersilyl moieties, and one phenylphosphine moiety. Its formation mechanism is very likely the same as that proposed for the analogous tetrafunctionalized anions $[Ge_9R_3Cr(CO)_3]^-$, in which a $\{Pd(PPh_3)\}$ fragment initially caps a trigonal-prismatic base of the anion **1** (tricapped trigonal prism).[3d] Such η^3-coordination has been observed for Pd sandwiched between two anions of **1** and for $\{Cu(PPh_3)\}$ capping the same anion.[8] In the case of **3**, the two prismatic bases of the parent **2** are different since one is ethyl decorated (atoms 1-2-3; Scheme 1 and Figure 1) and the opposite one is ligand free

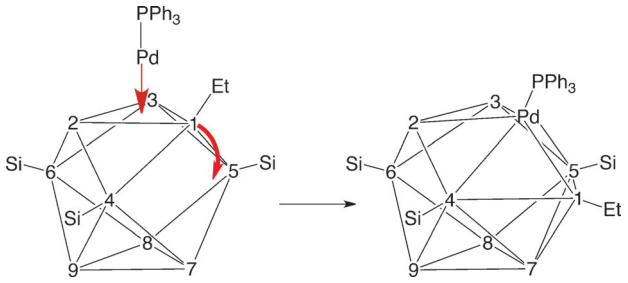

Scheme 1. A suggested mechanism for the formation of **3** (right) through capping of a triangular face of **2** by a $\{Pd(PPh_3)\}$ fragment, followed by displacement of the Et-bonded Ge vertex (atom 1).

(atoms 7-8-9). Relativistic DFT calculations (at the ZORA/PBE-TZ2P level employing relaxed structures without further simplification performed with the Amsterdam Density Functional (ADF) package[9]) show virtually no face preference for η^3-coordination based on the energy difference of 3.12 kcal mol^{-1}. Therefore, this cannot be the reason for the preference of the ethyl-decorated face. It is important to note, however, that based on the interaction energies of $\{Pd(PPh_3)\}$ with **1** and **2**, η^3-coordination is more favorable by about 184 kcal mol^{-1} for the neutral tetrasubstituted **2** compared to the same coordination for the trisubstituted anion **1**. This provides a good theoretical evaluation of the effect of the ethyl group and the zero charge of **2** on its chemistry and reactivity.

η^3-Coordination of the $\{Pd(PPh_3)\}$ fragment is then followed by "pushing" away of the {GeEt} motif, opening of the corresponding triangular face 1-2-3, and insertion of the fragment to achieve η^5-coordination within the cluster (Scheme 1). This rearrangement is favored by 33.3 kcal mol^{-1} for the ethyl-decorated face compared to the opposite ligand-free face, and this energy difference for the η^5-coordination is what defines the observed cluster compared to the one where the Pd fragment will be at the other available position. To recap, the ethyl group does not define the initial η^3-approach of the Pd fragment but dictates its final η^5-positioning.

The cluster rearrangement results in a much shorter 1–7 distance of 2.6817(7) Å compared to 3.634 Å in the parent trigonal prismatic **2**, where 1–7 is the longest prismatic edge (Scheme 1).[6b] Atom 1 and its ethyl substituent are now in the plane defined by the three Ge atoms bonded to hypersilyl substituents, that is, 4-5-6, positioning the ethyl group between two hypersilyl groups. The Pd–Ge distances for the three Ge atoms of the original triangular face, that is, atoms 1-2-3, are fairly short and in the range 2.4324(7) –2.5152 (8) Å, while the additional two interactions with atoms 4 and 5 are at relatively longer distances of 2.7166(5) and 2.7260(6) Å, respectively. Overall, the average Pd–Ge distance of 2.577 Å is virtually identical with that of the sandwiched and pseudo-octahedral palladium in $[(Ge_9R_3)Pd(Ge_9R_3)]^{2-}$ (2.568 Å)[8] and the η^4-coordinated palladium in $[Ge_9Pd\text{-}PPh_3]^{3-}$ (2.587 Å).[10]

The overall geometry of the $[Ge_9Pd]$ core in **3** can be viewed as a bicapped square antiprism where the Pd atom takes one of the square-antiprismatic sites and is 5-coordinate within the core. This positioning of the metal atom is unlike most of the known $[Ge_9M]$ clusters where the metal atom takes one of the two capping positions with η^4-coordination.[10,11] The two squares of the antiprism in **3** are made of atoms 4-5-7-Pd and 2-3-8-9, while the capping atoms are 1 and 6. The $[PdGe_3]$ square is noticeably smaller, with an average edge length of 2.762 Å compared to the $[Ge_4]$ square, which has an average edge length of 3.018 Å. The *exo* bonds to the five functionalities are unaffected upon insertion of the new palladium vertex. Overall, the cluster has a pseudo mirror plane cutting through atoms Pd-1-7-6.

The bonding of the $\{Pd(PPh_3)\}$ fragment in **3** (Figure 2) involves interactions between the palladium 4d and 4d/5s levels with the Ge_9 core-based orbitals. However, both the highest occupied and the lowest unoccupied orbitals in the new species are of mainly Ge_9 core character. The resulting sizable gap of about 1.66 eV suggests stability from the point of view of electronic structure. Hirshfeld charge analysis (see the Supporting Information) shows that there is a slight charge donation of 0.15 e$^-$ from the $\{Pd(PPh_3)\}$ fragment towards the Ge_9 core, and this is in line with the more electronegative character of the latter.

The core geometry of **3** is similar to that of the previously reported tetrafunctionalized anionic species $[Ge_9R_3M(CO)_3]^-$ (M = Cr, Mo, W) and the naked tetra-anions $[Sn_9W(CO)_3]^{4-}$ and $[Pb_9Mo(CO)_3]^{4-}$, all with inserted $\{M(CO)_3\}$ fragments.[3d,e,12] A similar example but with a $[Ge_8M_2]$ core has been reported in the tetra-anion $[Ge_8(Mo(CO)_3)_2]^{4-}$ as well.[13] It should be noted that the core of **3** is the first with a 5-connected transition metal other than from Group VI, the

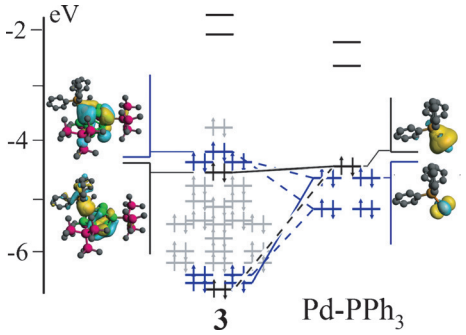

Figure 2. Schematic representation of the electronic structure of **3**, highlighting the contribution from the $\{Pd(PPh_3)\}$ fragment based orbitals. Colors for major participation in the occupied orbitals: blue for Pd 4d, black for Pd 4d/5s, and grey for the Ge_9 core. Isosurface plots of relevant molecular orbitals are shown.

first with a noble metal, and the first such cluster that is without charge.

The electron count of **3** is easily understood as a penta-functionalized *closo*-cluster that requires $2n+2=22$ cluster-bonding electrons for $n=10$ vertices.[14] These 22 electrons are provided by five naked germanium atoms (each contributes 2 electrons; the other 2 electrons are used for a lone pair), four *exo*-bonded germanium atoms (each contributes 3 electrons; the other 1 electron is used in the *exo* bond), and the {Pd(PPh_3)} fragment (contributes 0 cluster-bonding electrons since Pd is d^{10}; the pair of electrons for the *exo* bond comes from the ligand): $5\times2+4\times3+0=22$.

The new environment of the ethyl group in **3**, between two hypersilyl groups riding on a germanium vertex directly bonded to the inserted palladium, significantly affects its ^{1}H NMR chemical shift compared to **2**. Both the methylene and methyl protons are shifted downfield and are observed at $\delta=2.772$ and 2.046 ppm, respectively, in **3**, while in **2**, they are at $\delta=1.813$ and 1.467 ppm, respectively (Figures S1 and S2 in the Supporting Information). However, the most interesting feature is that the hypersilyl protons of **3** show two separate and sharp peaks in a ratio of 2:1, while there is only one broad signal in **2** (Figures S1 and S2). The latter splits into two at lower temperatures and sharpens at higher temperature, which is a classical indication of solution dynamics. The two sharp peaks in **3**, on the other hand, do not change even at the higher temperature of 75 °C (Figure S3). All of this suggests that **3** is static in solution, that is, the addition of the {Pd(PPh_3)} fragment quenches the mobility of the atoms observed in **2**. The ^{13}C NMR spectrum is also in agreement with this conclusion, showing two signals for the methyl groups of the hypersilyl substituents (Figure S4). Overall, the integrated proton signals in the ^{1}H NMR spectrum of **3** match its formula quite well, with 6.14:7.92:2.00:3.54:34.02:56.75 measured for 6H (phenyl), 9H (phenyl), 2H (CH_2), 3H (CH_3), 27H ($SiCH_3$), 54H (Si-CH_3), respectively, thus highlighting the fixed position of the hypersilyl ligands.

We have already stated before that the observed dynamic behavior of **2** is consistent with two possible intramolecular scenarios (we have shown that the dynamics is solution independent and therefore hypersilyl dissociation is unlikely). The first assumes nonlabile Ge–Si bonds and a highly fluid cluster core where the Ge atoms, together with their substituents, scramble somehow independently of the substituents. This mechanism, however, would predict an equally fluid and dynamic cluster **3**, and this is not the case. The second scenario assumes more labile Ge–Si bonds, which allow the three hypersilyl groups to migrate on the surface of the cluster. We speculated that the three hypersilyl groups rotate in a synchronized manner around the waist of the tricapped trigonal prismatic cluster core by switching from a single-atom-bonded position to a bridging position. Such rotation would be impossible in **3** because of the "insertion" of the ethyl substituent within the plane of rotation of the hypersilyl groups. We have now investigated this behavior computationally using simpler -SiH_3 substituents instead of hypersilyl groups. By using the transition-state search and vibrational analysis in the ADF package, we explored the potential energy surface in order to elucidate intermediates and transition states involved in the dynamic processes (Figure S5).[9] The results revealed a slightly different exchange mechanism. It involves similar bond–bridge–bond migration for the silyl groups, but along existing bonds as shown in Scheme 2 and Figures S5 and S6. The silyl groups bonded to atoms 4, 5, and 6 move to atoms 9, 7, and 3, respectively (Scheme 2). This is followed by a very small

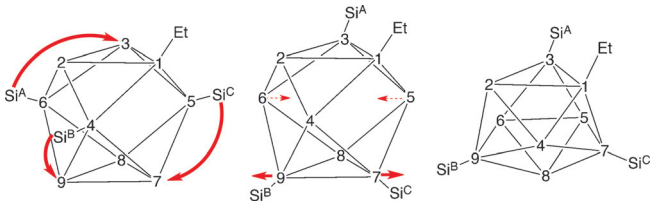

Scheme 2. A suggested mechanism for the dynamics observed in **2**.

cluster distortion where atoms 5 and 6 become closer while atoms 7 and 9 become further apart. This leads to a new tricapped trigonal prism where the bases are now 1-2-4 and 5-6-8, while the capping atoms are 3, 7, and 9. Note that while at the beginning, the silyl group labeled Si^A was in a different environment to the equivalent Si^B and Si^C, it is now Si^B that is different from the equivalent Si^A and Si^C (Scheme 2). These dynamics lead to the observed temperature dependence of the hypersilyl protons in the NMR spectra of compound **2**. The barrier for this migration in $EtGe_9(SiH_3)_3$ is calculated to be a very reasonable 4.5 kcal mol^{-1} and goes up for larger silyl substituents, for example, 7.3 kcal mol^{-1} for $EtGe_9(SiMe_3)_3$. For comparison, the measured barrier in compound **2** (with hypersilyl groups) is $\Delta G^{\ddagger}_{298}=14.1$ kcal mol^{-1} ($\Delta H^{\ddagger}=10.8$ kcal mol^{-1}; $\Delta S^{\ddagger}=4.6$ cal mol^{-1} K). Upon coordination of {Pd(PPh_3)}, such migration might be possible [10.6 kcal mol^{-1} is calculated for analogous migration of the silyl groups in $EtGe_9(SiMe_3)_3(PdPPh_3)$], but any cluster rearrangement similar to **2** is blocked by the position of the ethyl group and the ligated Pd vertex. There is no available pathway for hypersilyl migration that could account for averaging of the environments of all three hypersilyl groups.

Acknowledgements

We thank Dr. Allen G. Oliver for his help with the crystallography and also the financial donation by Dr. Joseph Y. Chang for partial support of this research. A.M.-C. thanks the support from FONDECYT 1140359 grant.

Keywords: cluster compounds · germanium · molecular dynamics · palladium · Zintl anions

How to cite: *Angew. Chem. Int. Ed.* **2016**, *55*, 8630–8633
Angew. Chem. **2016**, *128*, 8772–8775

[1] Reviews: a) S. C. Sevov, J. M. Goicoechea, *Organometallics* **2006**, *25*, 5678–5692; b) A. Schnepf, *Chem. Soc. Rev.* **2007**, *36*, 745–758; c) S. Scharfe, F. Kraus, S. Stegmaier, A. Schier, T. F.

Fässler, *Angew. Chem. Int. Ed.* **2011**, *50*, 3630 – 3670; *Angew. Chem.* **2011**, *123*, 3712 – 3754.
[2] A. Schnepf, *Angew. Chem. Int. Ed.* **2003**, *42*, 2624 – 2625; *Angew. Chem.* **2003**, *115*, 2728 – 2729.
[3] a) C. Schenk, A. Schnepf, *Angew. Chem. Int. Ed.* **2007**, *46*, 5314 – 5316; *Angew. Chem.* **2007**, *119*, 5408 – 5410; b) C. Schenk, F. Henke, G. Santiso-Quiñones, I. Krossing, A. Schenpf, *Dalton Trans.* **2008**, 4436 – 4441; c) F. Henke, C. Schenk, A. Schenpf, *Dalton Trans.* **2009**, 9141 – 9145; d) C. Schenk, A. Schnepf, *Chem. Commun.* **2009**, 3208 – 3210; e) F. Henke, C. Schenk, A. Schenpf, *Dalton Trans.* **2011**, *40*, 6704 – 6710.
[4] O. Kysliak, C. Schenk, A. Schnepf, *Angew. Chem. Int. Ed.* **2016**, *55*, 3216 – 3219; *Angew. Chem.* **2016**, *128*, 3270 – 3274.
[5] F. Li, S. C. Sevov, *Inorg. Chem.* **2012**, *51*, 2706 – 2708.
[6] a) F. Li, A. Muñoz-Castro, S. C. Sevov, *Angew. Chem. Int. Ed.* **2012**, *51*, 8581 – 8584; *Angew. Chem.* **2012**, *124*, 8709 – 8712; b) F. Li, S. C. Sevov, *J. Am. Chem. Soc.* **2014**, *136*, 12056 – 12063.
[7] a) F. S. Kocak, P. Y. Zavalij, Y.-F. Lam, B. W. Eichhorn, *Chem. Commun.* **2009**, 4197 – 4199; b) B. W. Eichhorn, S. Kocak, *Struct. Bonding (Berlin)* **2010**, *140*, 59 – 89; c) J. Q. Wang, S. Stegmaier, B. Wahl, T. F. Fässler, *Chem. Eur. J.* **2010**, *16*, 1793; d) E. N. Esenturk, J. Fettinger, B. Eichhorn, *Chem. Commun.* **2005**, 247.
[8] F. Li, S. C. Sevov, *Inorg. Chem.* **2015**, *54*, 8121 – 8125.
[9] Amsterdam Density Functional (ADF) Code, Vrije Universiteit, Amsterdam, The Netherlands, http://www.scm.com.
[10] Z.-M. Sun, Y.-F. Zhao, J. Li, L.-S. Wang, *J. Cluster Sci.* **2009**, *20*, 601 – 609.
[11] a) J. M. Goicoechea, S. C. Sevov, *J. Am. Chem. Soc.* **2006**, *128*, 4155 – 4161; b) J. M. Goicoechea, S. C. Sevov, *Organometallics* **2006**, *25*, 4530 – 4536; c) S. Scharfe, T. F. Fässler, *Eur. J. Inorg. Chem.* **2010**, 1207 – 1213; d) B.-B. Zhou, M. S. Denning, C. Jones, J. M. Goicoechea, *Dalton Trans.* **2009**, 1571 – 1578.
[12] a) B. Kesanli, J. Fettinger, B. W. Eichhorn, *Chem. Eur. J.* **2001**, *7*, 5277 – 5285; b) L. Yong, S. D. Hoffmann, T. F. Fässler, *Eur. J. Inorg. Chem.* **2005**, 3663 – 3669.
[13] Y. Wang, Q. Qin, J.-Y. Wang, R.-L. Sang, L. Xu, *Chem. Commun.* **2014**, *50*, 4181 – 4183.
[14] K. Wade, *Adv. Inorg. Chem. Radiochem.* **1976**, *18*, 1 – 66.

Received: April 6, 2016
Published online: May 31, 2016

